

Published in final edited form as:

*Biochem Biophys Res Commun.* 2008 October 17; 375(2): 225–229. doi:10.1016/j.bbrc.2008.08.010.

## WNK4 regulates the secretory pathway via which TRPV5 is targeted to the plasma membrane

Yi Jiang<sup>a,b</sup>, Peilong Cong<sup>a</sup>, Shawn R. Williams<sup>c</sup>, Wei Zhang<sup>a</sup>, Tao Na<sup>a</sup>, He-Ping Ma<sup>a</sup>, and Ji-Bin Peng<sup>a\*</sup>

<sup>a</sup>Nephrology Research and Training Center, Division of Nephrology, Department of Medicine, University of Alabama at Birmingham, Birmingham, AL 35294, USA

<sup>b</sup>Department of General Surgery, the Second Hospital of Jilin University, Changchun, Jilin 130041, China

<sup>c</sup>Department of Cell Biology, University of Alabama at Birmingham, Birmingham, AL 35294, USA

### Abstract

TRPV5 and TRPV6 are two closely related epithelial calcium channels that mediate apical calcium entry in the transcellular calcium transport pathway. TRPV5, but not TRPV6, is enhanced by protein kinase WNK4 when expressed in *Xenopus laevis* oocytes. We report that the majority of human TRPV5 exogenously expressed in the *Xenopus* oocyte plasma membrane was complexly *N*-glycosylated whereas that for human TRPV6 was core-glycosylated. Unglycosylated N358Q mutants of TRPV5 and TRPV6 were able to be expressed in the plasma membrane albeit with decreased abilities in mediating calcium uptake. Syntaxin 6, a SNARE protein in the *trans*-Golgi network, blocked the complex glycosylation of TRPV5 and TRPV6, rendered the channels in core-glycosylated form. Blocking complex glycosylation of TRPV5 either by syntaxin 6 or by N358Q mutation abolished the enhancing effect of WNK4 on TRPV5. Thus the difference in membrane expression of TRPV5 and TRPV6 explains the selective effect of WNK4 on TRPV5, which is likely on the secretory pathway involving complex glycosylation of channel proteins.

### Keywords

TRPV5; TRPV6; WNK4; syntaxin 6; *N*-glycosylation; calcium transport; epithelial calcium channels

### Introduction

Epithelial calcium (Ca<sup>2+</sup>) channels TRPV5 and TRPV6 (also known as ECaC and CaT1, respectively) are responsible for Ca<sup>2+</sup> entry in the transcellular pathways of Ca<sup>2+</sup> transport in the kidney and intestine, respectively [1;2]. While TRPV5 is restricted to the distal convoluted tubule and connecting tubule of the kidney [3], TRPV6 is more broadly distributed in the gastrointestinal tract, placenta, and some exocrine organs including the pancreas, prostate and salivary gland where it may participate in Ca<sup>2+</sup> transport and/or Ca<sup>2+</sup> signaling processes [4–6]. The two channels share 75% amino-acid sequence identity and are very similar in many

\*To whom correspondence should be addressed, Ji-Bin Peng, Ph.D., University of Alabama at Birmingham, Division of Nephrology, ZRB 625, 1900 University BLVD, Birmingham, AL 35294-0006, Tel: +1 (205) 975-6130, Fax: +1 (205) 996-2250, Email: jpeng@uab.edu.

**Publisher's Disclaimer:** This is a PDF file of an unedited manuscript that has been accepted for publication. As a service to our customers we are providing this early version of the manuscript. The manuscript will undergo copyediting, typesetting, and review of the resulting proof before it is published in its final citable form. Please note that during the production process errors may be discovered which could affect the content, and all legal disclaimers that apply to the journal pertain.

functional properties. Nevertheless,  $\text{Ca}^{2+}$  uptake and current mediated by human TRPV6 are much smaller than those mediated by human TRPV5 when they are expressed in *Xenopus laevis* oocytes [7]. Furthermore, WNK4, a protein serine/threonine kinase whose gene mutations cause familial hyperkalemic hypertension with hypercalciuria [8;9], specifically enhances TRPV5-mediated  $\text{Ca}^{2+}$  transport through increasing surface level of TRPV5 without a significant effect on TRPV6 [10]. In the present study, we aimed at the mechanism underlying the difference in the effects of WNK4 on TRPV5 and TRPV6 through analyzing the difference in TRPV5 and TRPV6 expression in the plasma membrane of *X. laevis* oocytes.

## Materials and Methods

### Plasmid constructs

The human TRPV5 and TRPV6 cDNAs were described previously [7]. Human syntaxin 6 cDNA was amplified from Caco-2 cells and was verified by sequencing. The human WNK4 cDNA was provided by Dr. Xavier Jeunemaitre. The cDNAs were subcloned into a homemade *X. laevis* oocytes expression vector pIN. An enhanced green fluorescent protein (EGFP) or a FLAG tag was incorporated into the amino-termini of TRPV5 and TRPV6 using a PCR approach for detecting TRPV5 and TRPV6 with confocal microscopy and Western blot analysis, respectively. N358Q mutants were generated using the QuikChange site-directed mutagenesis kit (Stratagene, La Jolla, CA, USA) following the manufacture's instruction. All the mutants were confirmed by sequencing.

### $\text{Ca}^{2+}$ uptake assay and two-microelectrode voltage clamp

*In vitro* transcription, injection of capped synthetic RNAs (cRNAs) into oocytes,  $\text{Ca}^{2+}$  uptake assay, and voltage clamp using oocytes were conducted as described previously [2;10]. The animal protocol used in this study was approved by the Institutional Animal Care and Use Committee (IACUC) of the University of Alabama at Birmingham. cRNA for TRPV5 was injected at 6.25 ng/oocyte, and 12.5 ng/oocyte for TRPV6, WNK4 and syntaxin 6. When a combination of 2 or 3 cRNAs was required, the concentrations of individual cRNAs were unaltered. Experiments were performed at 2 days after injection, and data are presented as means  $\pm$  S.E. of three or more experiments, with  $P < 0.05$  considered to be statistical significant.

### Surface Biotinylation and Western blot analysis

Two days after injection with cRNA, oocytes were washed with modified Barth's solution (MBS) for 5 times on ice, then incubated with 1 mg/ml Sulfo-NHS-SS-Biotin (Pierce Biotechnology, Rockford, IL, USA) in MBS at 4 °C for 1 hr with end to end shaking. Oocytes were washed 5 times then quenched with 100 mM glycine in MBS for 1 hr at 4 °C. Oocytes were lysed with lysis buffer (NaCl 100 mM, Tris-Cl 20 mM, Triton X100 1%, pH 7.6) and the yolk was removed by centrifuge at 3000 g for 10 min. Supernatants were then incubated with immobilized NeutrAvidin beads (Pierce) for 2 hrs at 4 °C. The beads were centrifuged and the supernatants were removed. The beads were washed 3 times with PBS. Biotinylated proteins were eluted from the beads by SDS-PAGE loading buffer with 50 mM DDT at 65 °C for 10 min. Both input cell lysates and biotinylated samples were subjected to SDS-PAGE. Proteins were transferred from the gel onto nitrocellulose membrane and blocked by 5% non-fat dry milk in PBS containing 0.05% Tween 20 (PBS-T) for 1 hr. FLAG-tagged TRPV5/6 proteins were probed by anti-FLAG antibody (Sigma-Aldrich, St. Louis, MO, USA) with 1:1000 dilution at 4°C overnight. After being washed with PBS-T for 5 min 4 times, the membrane was probed with HRP-conjugated goat anti rabbit secondary antibody (Pierce) with 1:1000 dilution at room temperature for 1 hr. The membrane was then washed with PBS-T for 5 min 4 times. TRPV5/6 signal was developed using SuperSignal West Pico chemiluminescent substrate (Pierce). Other antibodies were also used in Western blot analysis, including

antibodies against TRPV5 and WNK4 (Alpha Diagnostics International Inc., San Antonio, Texas, USA) and anti-syntaxin 6 antibody (BD Biosciences, San Jose, CA, USA).

### Confocal microscopy

*X. laevis* oocytes were injected with EGFP tagged TRPV5 or TRPV6 and were assayed with Leica SP1 DMIRBE laser-scanning confocal microscopy 2 days after injection. Excitation was performed at 488 nm with an argon laser and images were captured at an emission range of 500–600 nm using a 40× Plan Apo objective lens. Identical PMT and Offset parameters were applied to all measurements in the same experiments to maintain the same brightness and contrast settings for quantitative analysis. Images were captured at the equatorial plane of each oocyte.

### Glycosylation analysis

Lysates of *X. laevis* oocytes expressing TRPV5/6 were treated with peptide: *N*-glycosidase F (PNGase F) or endoglycosidase H (Endo H) following the manufacturer's instructions (New England Biolabs, Beverly, MA, USA). Equal amount of lysates were denatured at 65 °C for 10 min. After adding 1/10 volume of appropriate 10× reaction buffer (and 10% NP-40 for PNGase F reaction) and 2 μl (1000 units) of PNGase F, Endo H, or water (in control reactions), 40 μl samples were incubated at 37 °C for 1 to 2 hrs. After incubation, an equal volume of 2× sample buffer was added to each reaction. The resultant samples were then analyzed by SDS-PAGE and Western blot.

## Results

### TRPV5 and TRPV6 channel proteins expressed in the plasma membrane are at different *N*-glycosylation states

When expressed in *X. laevis* oocytes, human TRPV5-mediated Ca<sup>2+</sup> uptake and current were 1 to 4 times higher than those mediated by human TRPV6 [7;11]. The reason for this difference was unclear. Since both TRPV5 and TRPV6 are constitutively active, the level of mature channel proteins in the plasma membrane should determine their Ca<sup>2+</sup> transport activity. Indeed, when the EGFP-tagged TRPV5 or TRPV6 was expressed in *X. laevis* oocytes, EGFP-TRPV5 exhibited a sharper membrane distribution pattern (Fig. 1A), whereas EGFP-TRPV6 exhibited a diffused pattern (Fig. 1B). This suggests that a larger amount of EGFP-TRPV6 protein is distributed intracellular underneath the plasma membrane.

To further evaluate the plasma membrane expression of TRPV5 and TRPV6, the surface biotinylation approach was employed (Figs. 1C and D). A FLAG epitope was inserted in the amino-termini of TRPV5 and TRPV6 to compare the relative levels of TRPV5 and TRPV6 proteins using the immunoblot approach. No difference was observed between the FLAG tagged and untagged TRPV5/6 in expression and function aspects. TRPV5 and TRPV6 migrate in two major forms in SDS-PAGE; the higher band is complexly *N*-glycosylated and is resistant to Endo H, while the lower band is core-glycosylated and is sensitive to Endo H (Fig. 2) [10]. A much less intense band below the core-glycosylated band representing the unglycosylated form was also observed (Fig. 3A). Because the unglycosylated band was less intense and very close to the core-glycosylated band, it was often undetectable. Differences in plasma membrane expression of TRPV5 and TRPV6 were revealed by biotinylation experiments (Figs. 1C and D), which were performed under strict identical condition with the same batches of oocytes. Firstly, the intensity ratio between the complex glycosylated band and core-glycosylated band was much higher in TRPV5 than in TRPV6. Secondly, the majority of the surface biotinylated TRPV5 was in complex glycosylated form, whereas that for TRPV6 was in core-glycosylated form. Thirdly, the intensity of glycosylated band of TRPV5 was much higher than that of TRPV6. Fourthly, only a small fraction of the total protein (estimated ~2% of TRPV5 and

~0.5% of TRPV6) was biotinylated, suggesting that the majority of TRPV5 and TRPV6 are not present in the plasma membrane, even in the case of TRPV5 (Fig. 1A). These results indicate that TRPV6 is less effective in plasma membrane expression than TRPV5. This is likely due to the ineffective complex glycosylation of TRPV6 in the Golgi complex, which renders TRPV6 incapable of being efficiently delivered to the plasma membrane via the secretory pathway.

### TRPV5 and TRPV6 can reach the plasma membrane independent of N-glycosylation

Most TRPV5 proteins in the plasma membrane are in complex glycosylated form (Fig. 1C). To examine if complex glycosylation is required for TRPV5 to reach the plasma membrane, we removed the N-linked glycosylation site in TRPV5 and TRPV6. Human TRPV5 and TRPV6 possess only one N-linked glycosylation site; both are at asparagine 358 (N358). We therefore changed asparagine 358 into glutamine (N358Q) for both TRPV5 and TRPV6. The complexly glycosylated band was absent for N358Q mutants. Digestion with Endo H and PNGase F didn't change the band size of TRPV5/6<sup>N358Q</sup> (Fig. 2, left panel), indicating that TRPV5/6<sup>N358Q</sup> was indeed unglycosylated. Biotinylation study indicated that both N358Q mutants were capable of insertion to the plasma membrane (Figs. 1C and D). However, TRPV5<sup>N358Q</sup> and TRPV6<sup>N358Q</sup> exhibited 41.5 ± 1.9% and 30.0 ± 1.6 % reduction in Ca<sup>2+</sup> uptake (Fig. 2, right panel) and also reduced Na<sup>+</sup>-evolved current (Fig. 3C) compared to their respective wild-type (WT) proteins. This suggests that the function, the membrane expression of the channels, or both were affected by the removal of the sugar chain or simply by the mutation in N358. Because TRPV5 expressed in the plasma membrane is in complexly glycosylated form whereas TRPV6 reaches the plasma membrane in core-glycosylated form, it is not surprising that N358Q mutation appeared to affect TRPV5 more than TRPV6.

### Syntaxin 6 blocks the complex N-glycosylation of TRPV5 and TRPV6

After biosynthesis in the endoplasmic reticulum (ER), membrane proteins are processed in the ER and Golgi apparatus before insertion into the plasma membrane. N-linked core-glycosylation occurs in the ER, and complex glycosylation is completed in the Golgi apparatus. Since syntaxin 6 is a soluble N-ethylmaleimide-sensitive factor attachment protein receptor (SNARE) protein that is involved in vesicle trafficking in the secretory pathway [12;13], we examined the effect of syntaxin 6 on TRPV5 and TRPV6. Interestingly, exogenous expression of syntaxin 6 completely blocked the complex glycosylation of TRPV5 and TRPV6, and the majority of TRPV5 and TRPV6 proteins were in core-glycosylated state (Fig. 3A). The core-glycosylated form of TRPV5 and TRPV6 could reach the plasma membrane in the presence of syntaxin 6. Nevertheless, the TRPV5- and TRPV6-mediated Ca<sup>2+</sup> uptake values (Fig. 3B) and currents (Fig. 3C) were reduced by syntaxin 6 to extents similar to those of the N358Q mutants.

### The effect of WNK4 on TRPV5 is abolished by N358Q mutation or by coexpression of syntaxin 6

We have recently observed that WNK4 enhanced Ca<sup>2+</sup> transport mediated by TRPV5 but not that mediated by TRPV6 [10]. Western blot analysis revealed that the intensity of the complex glycosylated TRPV5 was increased by WNK4; this resulted in an increase in abundance of TRPV5 channel proteins in the cell surface [10]. TRPV6 was poorly complex glycosylated and reached the plasma membrane mainly in the core-glycosylated form (Fig. 1D). Since WNK4 specifically increases the level of complex glycosylated TRPV5, this may explain why WNK4 exhibited no significant effect on TRPV6. If this hypothesis is valid, it is expected that the effect of WNK4 will be diminished by N358Q mutation and/or by syntaxin 6, which blocks the complex glycosylation of TRPV5 (Fig. 3A). Indeed, WNK4 didn't increase Ca<sup>2+</sup> uptake mediated by TRPV6 in the presence of syntaxin 6 or by TRPV6<sup>N358Q</sup> (Fig. 4). Western blot

analysis revealed that the complex glycosylated form of TRPV5 was absent when syntaxin 6 was coexpressed even in the presence of WNK4 (Fig. 4). This suggests that the action of WNK4 on TRPV5 likely occurs on or after the step of complex glycosylation. The selective effect of WNK4 on TRPV5 over TRPV6 is likely due to the fact that TRPV6 was poorly complex glycosylated and reached the plasma membrane mainly in core-glycosylated form through an alternative route to the secretory pathway.

## Discussion

WNK4 is a multifunctional protein that acts on ion transporters and channels through different mechanisms. For instance, WNK4 inhibits the thiazide sensitive  $\text{Na}^+\text{-Cl}^-$  cotransporter (NCC) through protein interaction [14–16], and likely via enhanced degradation of NCC by a lysosomal pathway [17]. On the other hand, WNK4 inhibits the renal outer medullary  $\text{K}^+$  channel (ROMK) through a clathrin-dependent endocytosis pathway [18]. Among all the ion transport proteins in the transcellular ion transport pathways regulated by WNK4 [19], TRPV5 is the only one that is enhanced by WNK4 [10]. We now provide evidence that the action of WNK4 on TRPV5 is likely in the secretory pathway for TRPV5 delivery to the plasma membrane.

Despite many similarities of TRPV5 and TRPV6, TRPV6 exhibited a lower efficiency of membrane expression and the majority of channel proteins in the plasma membrane were in core-glycosylated form. This suggests that unlike TRPV5, most of TRPV6 reside in the ER or Golgi complex after biosynthesis without going through a secretory pathway via *trans*-Golgi network to reach the plasma membrane. WNK4 increases the complex glycosylated TRPV5, which is likely on its way to the plasma membrane through the secretory pathway [10]. In the presence of syntaxin 6, the secretory pathway of TRPV5 is blocked; although a small portion of TRPV5 channel proteins reached the plasma membrane via a route bypassing the secretory pathway as what likely occurs to TRPV6. Thus it is likely that WNK4 facilitates the transport of TRPV5 through the secretory pathway to the plasma membrane without effecting an alternative route bypassing the secretory pathway via which TRPV6 (also TRPV5<sup>N358Q</sup> and TRPV5 in the presence of syntaxin 6) reaches the plasma membrane.

As in the case of ENaC [20], only a small fraction of total TRPV5 or TRPV6 proteins were present in the plasma membrane of *X. laevis* oocytes. This could be a result of over-expression of the channel proteins. However, some proteins of the TRPV family such as TRPV1, TRPV2, and TRPV3 exhibited plasma membrane localization when transfected into human embryonic kidney (HEK) 293 cells while the majority of the TRPV5 and TRPV6 channel proteins were intracellularly localized [21]. Our observation that only a small fraction of the protein was expressed in the oocyte plasma membrane is consistent with the aforementioned findings in mammalian cells. Intracellular localization of TRPV6 was reported in mouse tissues, especially in the pancreatic acinar cells [6]. TRPV5 was also intracellularly localized in the connecting tubule of the kidney [3]. Unlike some other channels of the TRPV family that are activated by chemical (such as ligand capsaicin for TRPV1) and/or physical (such as heat for TRPV1/2/3) stimuli, TRPV5 and TRPV6 are constitutively active once they reach the plasma membrane. Thus intracellularly localized channel proteins may serve as a reservoir for rapid increases of channel activity in the plasma membrane when needed. This is especially important for TRPV6 in exocrine function (e.g. in pancreatic acinar cells). This may explain why TRPV6 exhibited more profound intracellular localization compared to TRPV5 (Fig. 1).

To our knowledge, the effect of syntaxin 6 on blocking complex glycosylation of a membrane protein has not been reported previously. Syntaxin 6 is a SNARE protein with promiscuous behavior taking parts in different fusion events in *trans*-Golgi network [13], immature secretory granules, and endosomes [22]. Syntaxin 6 may affect both exocytosis and endocytosis

pathways [22;23]. For instance, it regulates trafficking of glucose transporter-4 (Glut4) in adipocytes [24], and modulates caveolar endocytosis [25]. The mechanism by which syntaxin 6 regulates TRPV5 and TRPV6 is unclear. A likely scenario is that most of the core-glycosylated TRPV5 and TRPV6 are trapped in the ER or Golgi complex without reaching the cisternae for complex glycosylation in the presence of excessive syntaxin 6. The exact mechanism of the action of syntaxin 6 on TRPV5 and TRPV6 warrants further study.

## Acknowledgements

This work was supported by a Scientist Development Grant (0430125N) from the American Heart Association and a grant (R01DK072154) from the National Institute of Diabetes and Digestive and Kidney Diseases. We thank Drs. Xavier Jeunemaitre and Juliette Hadchouel for the WNK4 cDNA.

## References

1. Hoenderop JG, van der Kemp AW, Hartog A, van de Graaf SF, Van Os CH, Willems PH, Bindels RJ. Molecular identification of the apical  $\text{Ca}^{2+}$  channel in 1,25-dihydroxyvitamin  $\text{D}_3$ -responsive epithelia. *J.Biol.Chem* 1999;274:8375–8378. [PubMed: 10085067]
2. Peng J-B, Chen X-Z, Berger UV, Vassilev PM, Tsukaguchi HT, Brown EM, Hediger MA. Molecular cloning and characterization of a channel-like transporter mediating intestinal calcium absorption. *J.Biol.Chem* 1999;274:22739–22746. [PubMed: 10428857]
3. Loffing J, Loffing-Cueni D, Valderrabano V, Klausli L, Hebert SC, Rossier BC, Hoenderop JG, Bindels RJ, Kaissling B. Distribution of transcellular calcium and sodium transport pathways along mouse distal nephron. *Am.J.Physiol Renal Physiol* 2001;281:F1021–F1027. [PubMed: 11704552]
4. Peng JB, Chen XZ, Berger UV, Vassilev PM, Brown EM, Hediger MA. A Rat Kidney-specific Calcium Transporter in the Distal Nephron. *J.Biol.Chem* 2000;275:28186–28194. [PubMed: 10875938]
5. Peng J-B, Chen X-Z, Berger UV, Weremowicz S, Morton CC, Vassilev PM, Brown EM, Hediger MA. Human calcium transport protein CaT1. *Biochem.Biophys.Res.Commun* 2000;278:326–332. [PubMed: 11097838]
6. Zhuang L, Peng JB, Tou L, Takanaga H, Adam RM, Hediger MA, Freeman MR. Calcium-selective ion channel, CaT1, is apically localized in gastrointestinal tract epithelia and is aberrantly expressed in human malignancies. *Lab Invest* 2002;82:1755–1764. [PubMed: 12480925]
7. Peng JB, Brown EM, Hediger MA. Structural conservation of the genes encoding CaT1, CaT2, and related cation channels. *Genomics* 2001;76:99–109. [PubMed: 11549322]
8. Wilson FH, Disse-Nicodeme S, Choate KA, Ishikawa K, Nelson-Williams C, Desitter I, Gunel M, Milford DV, Lipkin GW, Achard JM, Feely MP, Dussol B, Berland Y, Unwin RJ, Mayan H, Simon DB, Farfel Z, Jeunemaitre X, Lifton RP. Human hypertension caused by mutations in WNK kinases. *Science* 2001;293:1107–1112. [PubMed: 11498583]
9. Mayan H, Vered I, Mouallem M, Tzadok-Witkon M, Pauzner R, Farfel Z. Pseudohypoadosteronism type II: marked sensitivity to thiazides, hypercalciuria, normomagnesemia, and low bone mineral density. *J.Clin.Endocrinol.Metab* 2002;87:3248–3254. [PubMed: 12107233]
10. Jiang Y, Ferguson WB, Peng JB. WNK4 enhances TRPV5-mediated calcium transport: potential role in hypercalciuria of familial hyperkalemic hypertension caused by gene mutation of WNK4. *Am.J.Physiol Renal Physiol* 2007;292:F545–F554. [PubMed: 17018846]
11. Vassilev PM, Peng JB, Hediger MA, Brown EM. Single-channel activities of the human epithelial  $\text{Ca}^{2+}$  transport proteins CaT1 and CaT2. *J.Membr.Biol* 2001;184:113–120. [PubMed: 11719848]
12. Bock JB, Lin RC, Scheller RH. A new syntaxin family member implicated in targeting of intracellular transport vesicles. *J.Biol.Chem* 1996;271:17961–17965. [PubMed: 8663448]
13. Bock JB, Klumperman J, Davanger S, Scheller RH. Syntaxin 6 functions in trans-Golgi network vesicle trafficking. *Mol.Biol.Cell* 1997;8:1261–1271. [PubMed: 9243506]
14. Yang CL, Angell J, Mitchell R, Ellison DH. WNK kinases regulate thiazide-sensitive Na-Cl cotransport. *J.Clin.Invest* 2003;111:1039–1045. [PubMed: 12671053]

15. Yang CL, Zhu X, Wang Z, Subramanya AR, Ellison DH. Mechanisms of WNK1 and WNK4 interaction in the regulation of thiazide-sensitive NaCl cotransport. *J.Clin.Invest* 2005;115:1379–1387. [PubMed: 15841204]
16. Wilson FH, Kahle KT, Sabath E, Lalioti MD, Rapson AK, Hoover RS, Hebert SC, Gamba G, Lifton RP. Molecular pathogenesis of inherited hypertension with hyperkalemia: the Na-Cl cotransporter is inhibited by wild-type but not mutant WNK4. *Proc.Natl.Acad.Sci.U.S.A* 2003;100:680–684. [PubMed: 12515852]
17. Cai H, Cebotaru V, Wang YH, Zhang XM, Cebotaru L, Guggino SE, Guggino WB. WNK4 kinase regulates surface expression of the human sodium chloride cotransporter in mammalian cells. *Kidney Int* 2006;69:2162–2170. [PubMed: 16688122]
18. Kahle KT, Wilson FH, Leng Q, Lalioti MD, O'Connell AD, Dong K, Rapson AK, MacGregor GG, Giebisch G, Hebert SC, Lifton RP. WNK4 regulates the balance between renal NaCl reabsorption and K<sup>+</sup> secretion. *Nat.Genet* 2003;35:372–376. [PubMed: 14608358]
19. Peng JB, Warnock DG. WNK4-mediated regulation of renal ion transport proteins. *Am.J.Physiol Renal Physiol* 2007;293:F961–F973. [PubMed: 17634397]
20. Valentijn JA, Fyfe GK, Canessa CM. Biosynthesis and processing of epithelial sodium channels in *Xenopus* oocytes. *J.Biol.Chem* 1998;273:30344–30351. [PubMed: 9804797]
21. Hellwig N, Albrecht N, Harteneck C, Schultz G, Schaefer M. Homo- and heteromeric assembly of TRPV channel subunits. *J.Cell Sci* 2005;118:917–928. [PubMed: 15713749]
22. Wendler F, Tooze S. Syntaxin 6: the promiscuous behaviour of a SNARE protein. *Traffic* 2001;2:606–611. [PubMed: 11555414]
23. Misura KM, Bock JB, Gonzalez LC Jr, Scheller RH, Weis WI. Three-dimensional structure of the amino-terminal domain of syntaxin 6, a SNAP-25 C homolog. *Proc.Natl.Acad.Sci.U.S.A* 2002;99:9184–9189. [PubMed: 12082176]
24. Perera HK, Clarke M, Morris NJ, Hong W, Chamberlain LH, Gould GW. Syntaxin 6 regulates Glut4 trafficking in 3T3-L1 adipocytes. *Mol.Biol.Cell* 2003;14:2946–2958. [PubMed: 12857877]
25. Choudhury A, Marks DL, Proctor KM, Gould GW, Pagano RE. Regulation of caveolar endocytosis by syntaxin 6-dependent delivery of membrane components to the cell surface. *Nat.Cell Biol* 2006;8:317–328. [PubMed: 16565709]

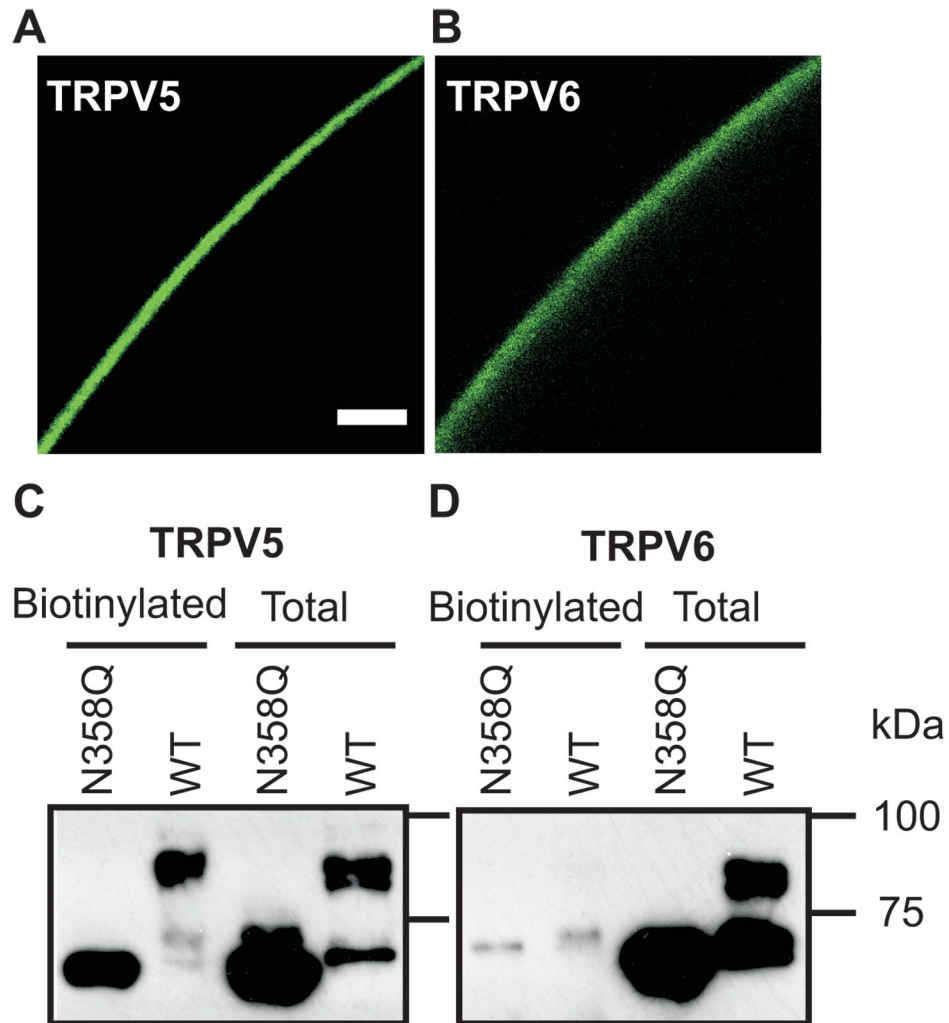


**Figure 1.** Difference in plasma membrane expression of TRPV5 and TRPV6 in *X. laevis* oocytes. **A** and **B.** Different distribution of EGFP tagged TRPV5 and TRPV6 in *X. laevis* oocytes revealed by Leica SP1 confocal microscopy. Bar denotes 25  $\mu$ m. **C** and **D.** Surface biotinylated TRPV5 and TRPV6 were in different glycosylated states. Glycosylation deficient N358Q mutants of TRPV5 and TRPV6 were employed as unglycosylated controls. Both proteins were tagged with FLAG in the N-terminal for detection with anti-FLAG antibody. Surface biotinylated proteins from 60 oocytes expressing individual proteins were isolated. In the biotinylated group (Biotinylated), proteins corresponding to 20 oocytes were loaded in each lane; in the total cell lysate (Total), proteins corresponding to 1 oocyte were loaded in each lane.



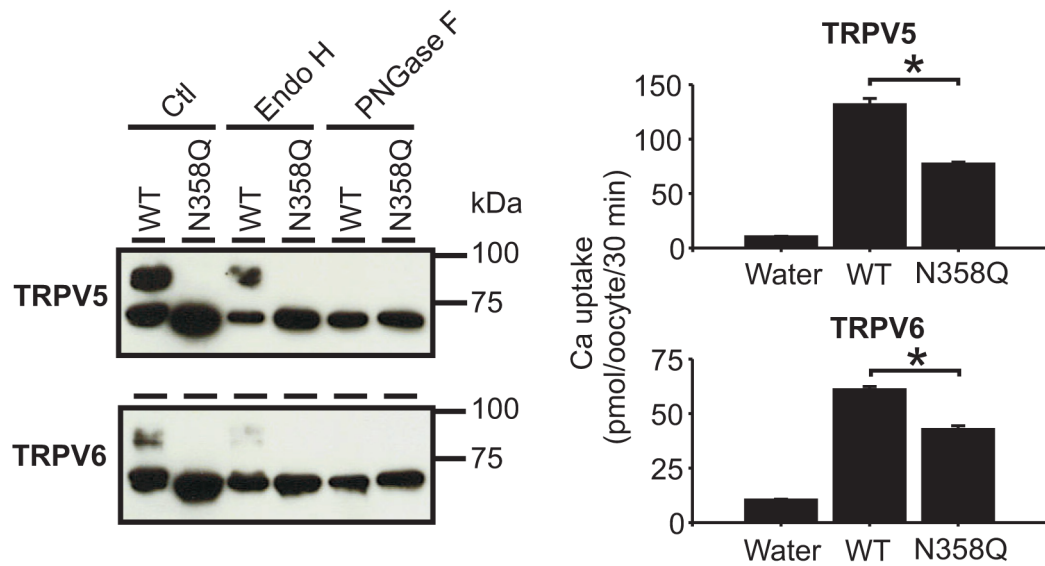


**Figure 2.** N358Q mutation in TRPV5 and TRPV6 abolished glycosylation of the channel proteins. *Left panel*, equal amount of *X. laevis* oocyte lysates containing wild-type (WT) or N358Q mutant of TRPV5 and TRPV6 were digested with Endo H and PNGase F and analyzed by Western blot. *Right panel*, Ca<sup>2+</sup> uptake activities of the N358Q mutants were decreased compared to the WT channels. \* indicates  $P < 0.05$  vs. WT group by Student's *t*-test.

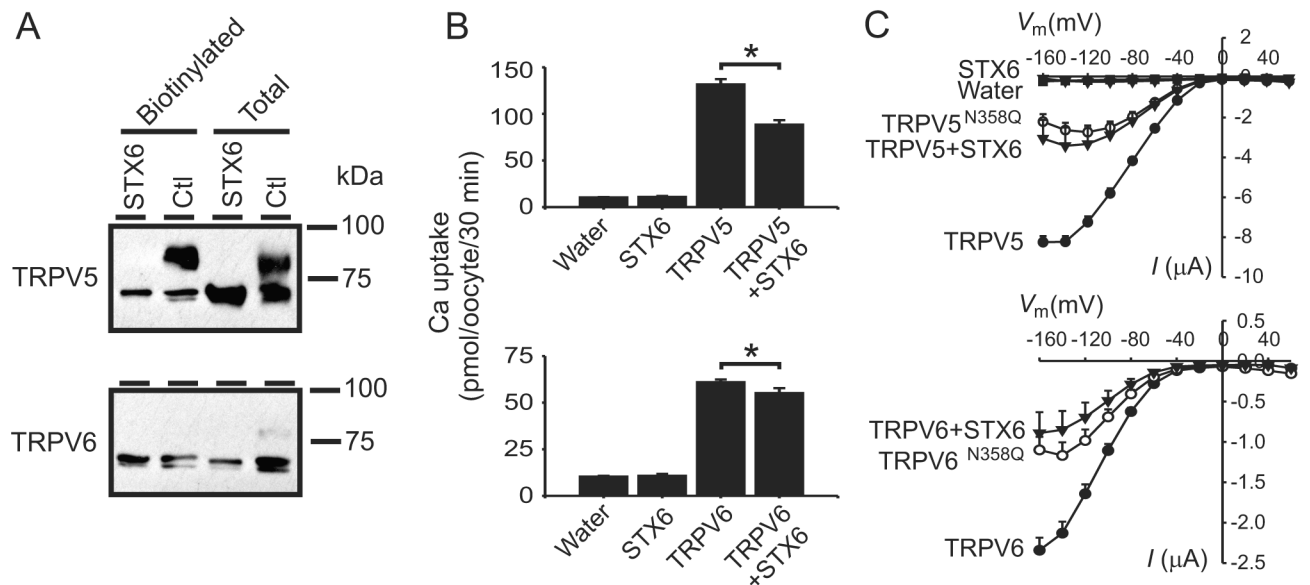


**Figure 3.**

Syntaxin 6 (STX6) blocks the complex glycosylation of TRPV5 and TRPV6. **A**, Complex glycosylation of TRPV5 and TRPV6 were blocked by co-expression of STX6. Surface biotinylation experiments indicated both TRPV5 and TRPV6 reach plasma membrane in core-glycosylated form in the presence of STX6. The lowest bands represent unglycosylated proteins. **B**, Ca<sup>2+</sup> uptake activities of TRPV5 and TRPV6 were significantly decreased by co-expression of syntaxin 6. \* indicates  $P < 0.05$ . **C**, Na<sup>+</sup>-evoked currents in control oocytes injected with water, or oocytes expressing TRPV5/6, TRPV5/6<sup>N358Q</sup> or TRPV5/6 with STX6. Voltage pulses between -160 and +60 mV, in increments of 20 mV, were applied, and steady-state currents were recorded. Na<sup>+</sup>-evoked currents were obtained by subtracting the current in the absence of NaCl from that in the presence of NaCl (100 mM). Standard perfusion solution contained (in mM) choline-Cl (or NaCl) 100, KCl 2, MgCl<sub>2</sub> 1 and HEPES 10, pH 7.5 (adjusted using Trisbase and HCl). Data were from 12 to 18 oocytes derived from three frogs.

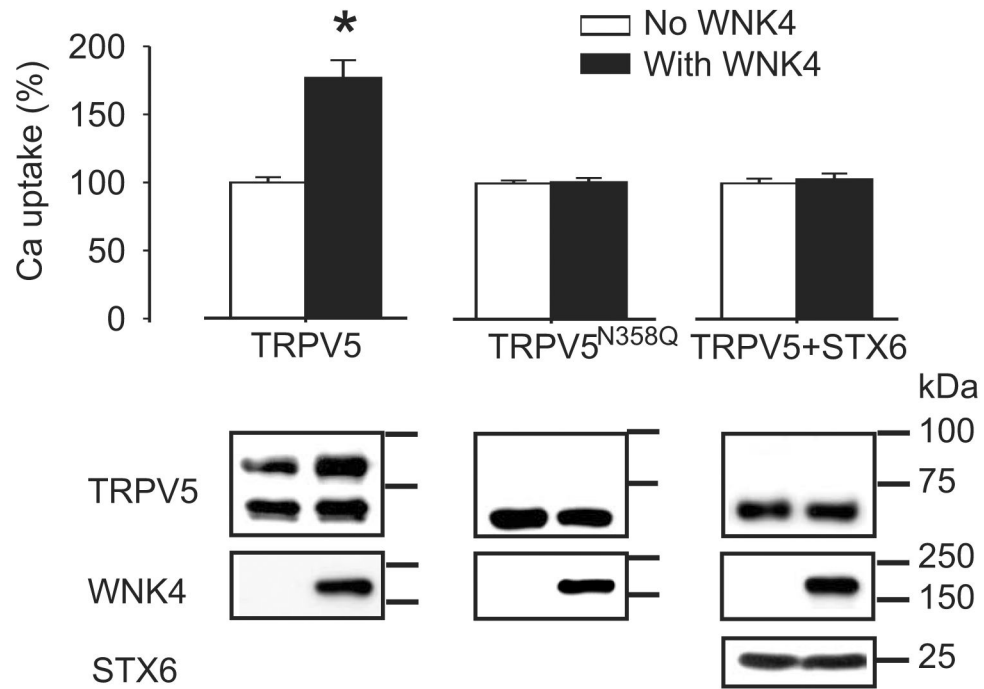


**Figure 4.** The enhancing effect of WNK4 on TRPV5 was blocked by the presence of STX6, or by removal of the glycosylation site in TRPV5 (TRPV5<sup>N358Q</sup>). Proteins involved were detected using antibodies against them with Western blot analysis (*lower panel*). Data are expressed as percentage of the mean value of the group without WNK4 in each set. \* indicates  $P < 0.05$ .